Soil Biology & Biochemistry 73 (2014) 69–83

Contents lists available at ScienceDirect

Soil Biology & Biochemistry

journal homepage: www.elsevier.com/locate/soilbio

A theoretical analysis of microbial eco-physiological and diffusion limitations to carbon cycling in drying soils

S. Manzoni [a,b,c,*], S.M. Schaeffer [d], G. Katul [e,f], A. Porporato [e,f], J.P. Schimel [g]

[a] Department of Crop Production Ecology, Swedish University of Agricultural Sciences, Uppsala, Sweden
[b] Department of Ecology, Swedish University of Agricultural Sciences, Uppsala, Sweden
[c] Department of Physical Geography and Quaternary Geology, Stockholm University, Sweden
[d] Department of Biosystems Engineering & Soil Science, University of Tennessee, Knoxville, TN, USA
[e] Nicholas School of the Environment, Duke University, Durham, NC, USA
[f] Department of Civil and Environmental Engineering, Duke University, Durham, NC, USA
[g] Department of Ecology, Evolution and Marine Biology, University of California at Santa Barbara, Santa Barbara, CA, USA

ARTICLE INFO

Article history:
Received 15 November 2013
Received in revised form
6 February 2014
Accepted 8 February 2014
Available online 26 February 2014

Keywords:
Soil moisture
Heterotrophic respiration
Decomposition
Microbial biomass
Dormancy
Osmoregulation
Water stress

ABSTRACT

Soil microbes face highly variable moisture conditions that force them to develop adaptations to tolerate or avoid drought. Drought conditions also limit the supply of vital substrates by inhibiting diffusion in dry conditions. How these biological and physical factors affect carbon (C) cycling in soils is addressed here by means of a novel process-based model. The model accounts for different microbial response strategies, including different modes of osmoregulation, drought avoidance through dormancy, and extra-cellular enzyme production. Diffusion limitations induced by low moisture levels for both extracellular enzymes and solutes are also described and coupled to the biological responses. Alternative microbial life-history strategies, each encoded in a set of model parameters, are considered and their effects on C cycling assessed both in the long term (steady state analysis) and in the short term (transient analysis during soil drying and rewetting). Drought resistance achieved by active osmoregulation requiring large C investment is not useful in soils where growth in dry conditions is limited by C supply. In contrast, dormancy followed by rapid reactivation upon rewetting seems to be a better strategy in such conditions. Synthesizing more enzymes may also be advantageous because it causes larger accumulation of depolymerized products during dry periods that can be used upon rewetting. Based on key model parameters, a spectrum of life-history strategies thus emerges, providing a possible classification of microbial responses to drought.

1. Introduction

The availability of water in soils is highly variable, depending on random rainfall inputs interspaced by dry periods (Rodriguez-Iturbe and Porporato, 2004). This variability affects soil microbes by creating pulses in activity after rainfall, but periods of limited activity when water is unavailable (Austin et al., 2004; Borken and Matzner, 2009). Due to the interactions among microbes, substrates, and water availability, and the timing of rainfall, microbial responses to drought and wetting events are nonlinear. Hence, even small increases in soil moisture after a long dry period may trigger a large respiration pulse. Because these pulsing dynamics may contribute a large fraction of ecosystem respiration (Reichstein et al., 2002; Carbone et al., 2011), including them in process-based models that can effectively predict respiration responses to current and altered hydro-climatic conditions is becoming necessary.

Disentangling physical and biological drivers of respiration pulses and microbial activity is complicated because they are interrelated (Or et al., 2007; Schimel et al., 2007; Moyano et al., 2013). On the one hand, solute diffusivity decreases as the soil becomes drier due to reduced water-filled porosity and increased tortuosity of the water films around solid particles (Skopp et al., 1990; Moldrup et al., 2001). As a result, diffusivity approaches near-zero as soil moisture reaches a point where water films become disconnected. On the other hand, soil matric potentials become more negative, potentially requiring osmotic adjustments for microbial cells to maintain turgor and function (Welsh, 2000; Schimel

* Corresponding author. Swedish University of Agricultural Sciences, Department of Crop Production Ecology, Box 7043, Ulls väg 16, Uppsala, Sweden. Tel.: +46 (0)18 671418.
E-mail address: stefano.manzoni@slu.se (S. Manzoni).

http://dx.doi.org/10.1016/j.soilbio.2014.02.008
0038-0717/

et al., 2007). The osmolyte demand, however, might not be met in dry soils due to limited substrate availability (Boot et al., 2013; Kakumanu et al., 2013). In such conditions, switching to a dormant state could be a successful strategy (or the only option), allowing microbes to avoid drought and await moister conditions to resume metabolic activity.

Dormancy may be a useful strategy to maintain a functional and diverse microbial community in the long term (Bär et al., 2002; Jones and Lennon, 2010). However, dormancy may result in delayed recovery of activity upon rewetting (Placella et al., 2012), possibly causing inefficient use of resources that are rapidly made available immediately after a rainfall event. It is also conceivable that extra-cellular enzyme production could be tuned to maximize C uptake (Vetter et al., 1998; Allison, 2012; Moorhead et al., 2012). In drying soils where microbial activity is low, extra-cellular enzymes may still be able to degrade organic matter, causing bioavailable substrates to accumulate, until they become available upon rewetting (Lawrence et al., 2009; Zeglin et al., 2013). Changing the rate and timing of extra-cellular enzyme synthesis could affect these dynamics and certain patterns could maximize the benefits for the microbes.

The presence of this tradeoff between the contrasting needs of surviving drought and being active when resources are available raises the question as to how these strategies (dormancy *vs.* drought resistance) are coupled with C allocation in microbes (osmoregulation and enzyme synthesis) and ultimately affect soil C storage and respiration pulses. Considering the wide range of microbial responses to drought that has been observed (Freckman, 1986; Lennon et al., 2012), it is conceivable that different microbial communities may employ different strategies depending on the rainfall regime. Here, three eco-physiological modes of response that shape a range of life-history strategies are considered. How each mode functions under varying moisture regimes is evaluated for i) osmoregulation, ii) dormancy/reactivation, and iii) extra-cellular enzyme synthesis. Despite a large degree of flexibility in these strategies, physical limits to acclimation exist (e.g., limited soil and substrate diffusivity) that might constrain the possible range of responses (Manzoni et al., 2012). The question of how these physical processes and physiological responses interact to originate the observed respiration–soil moisture relation has not yet been fully addressed. Here, this question is addressed from a theoretical perspective using a novel process-based soil biogeochemical model that accounts for key physical constraints and physiological responses to drought.

Current soil biogeochemical models employ empirical kinetic rate modifiers to account for soil moisture effects on microbial respiration (Rodrigo et al., 1997; Bauer et al., 2008; Moyano et al., 2012). Typically, these modifiers increase from zero at a lower soil moisture threshold to a unitary value around the soil field capacity or at soil saturation (Manzoni and Porporato, 2007; Lawrence et al., 2009). Other models describe respiration as a function of substrate and oxygen availabilities, which are linked to soil moisture via empirical diffusivity functions (Skopp et al., 1990; Schjonning et al., 2003; Davidson et al., 2012). While accounting in part for diffusion constraints, these models neglect microbial physiological responses to water limitation, and hence cannot capture the mechanistic drivers of the respiration–moisture and soil C–moisture relations.

To provide a description of these processes that captures physiological mechanisms of moisture/drought response, a physiologically-based soil C model accounting for solute diffusion limitations and the dynamics of osmoregulation and dormancy is proposed. Using this model, we first investigate how physiological traits and strategies (osmoregulation, dormancy/reactivation, enzyme production) and physical constraints (diffusivity) control the long-term partitioning of soil C among different pools along moisture gradients. Next, how these biological and physical constraints alter the shape of the respiration–moisture relation and C allocation in microbes during drying and rewetting cycles is assessed.

2. Theory

2.1. Model structure

To focus on the microbial responses to soil moisture variations, soil carbon (C) pools and fluxes only are considered, assuming that nutrients are not limiting. Compartments are expressed as g C m^{-3} of soil and fluxes as g C m^{-3} d^{-1} (full lists of symbols and their units are reported in Tables 1 and 2). The model is to be interpreted at the daily time scale, allowing the elimination of some processes that occur at faster scales. We also focus on the effects of water availability and neglect temperature effects. The proposed model is lumped in space, so that respiration on an area basis (g C m^{-2} d^{-1}) is simply obtained by multiplying the respiration flux by the mean soil depth (Z_r). The model builds on the structure proposed by Schimel and Weintraub (2003), which includes soil organic matter substrates (C_S), soluble organic substrates (C_D), microbial biomass (C_B), and enzyme pools (C_E) (variables and fluxes are defined in Fig. 1). Here, a compartment of dormant biomass ($C_{B,D}$) and two compartments for intra-cellular osmolytes in the active and dormant biomass (C_O and $C_{O,D}$, respectively) are added to improve the description of water stress physiology. We emphasize that

Table 1
List of variables, fluxes, physiological functions, transfer and diffusion coefficients, and other variable quantities. In Fig. 8, subscript T indicates time-integrated quantities over the whole drying period.

Symbol	Description	Units
A/V	Ratio of area around the microbial cells over volume of soil surrounding them	m^{-1}
c	Osmolyte concentration in cytoplasmic free water	mol m^{-3}
C_B	C in active microbial biomass	gC m^{-3}
$C_{B,D}$	C in dormant microbial biomass	gC m^{-3}
C_D	Soluble organic C	gC m^{-3}
C_E	Enzymatic C	gC m^{-3}
C_O	Osmolyte C in active microbial biomass	gC m^{-3}
$C_{O,D}$	Osmolyte C in dormant microbial biomass	gC m^{-3}
C_S	Stable soil organic C substrates	gC m^{-3}
D	Decomposition rate	gC m^{-3} d^{-1}
D_D	Diffusivity of dissolved organic C in bulk soil	m^2 s^{-1}
D_E	Diffusivity of enzymes in bulk soil	m^2 s^{-1}
$f_{A\to D}$	Switching function for active-dormant state transition	–
$f_{D\to A}$	Switching function for dormant-active state transition	–
h_D	Transfer coefficient for dissolved organic C	d^{-1}
h_E	Transfer coefficient for enzymes	d^{-1}
E_P	Enzyme production rate	gC m^{-3} d^{-1}
ET	Evapotranspiration rate	m d^{-1}
I	Rainfall rate	m d^{-1}
I_L	Litterfall rate	gC m^{-3} d^{-1}
M_B	Mortality of active microbial biomass	gC m^{-3} d^{-1}
$M_{B,D}$	Mortality of dormant microbial biomass	gC m^{-3} d^{-1}
$P_{A\to D}$	Transfer from active to dormant population	gC m^{-3} d^{-1}
$P_{D\to A}$	Transfer from dormant to active population	gC m^{-3} d^{-1}
L	Deep percolation rate	m d^{-1}
L_D	Leaching of dissolved organic C	gC m^{-3} d^{-1}
L_E	Leaching of enzymes	gC m^{-3} d^{-1}
R_G	Growth respiration	gC m^{-3} d^{-1}
R_M	Maintenance respiration	gC m^{-3} d^{-1}
U	Microbial uptake	gC m^{-3} d^{-1}
s	Relative volumetric soil moisture	–
φ	Coefficient for increased transition to dormancy under limited C supply	–
Π	Osmolyte allocation	gC m^{-3} d^{-1}
ψ	Soil matric potential	MPa
Ω_B	Osmotic potential of the microbial cell, $\Omega_B=\psi-\pi_B$	MPa

osmolyte pools are described separately from the other components of microbial biomass (included in C_B); therefore, the total microbial pool as would be measured by fumigation extraction is given by $C_B + C_{B,D} + C_O + C_{O,D}$.

Soil organic C receives a litterfall input (I_L) and is decomposed (D) by enzymatic reactions to soluble compounds that feed the C_D compartment. Microbes take up these compounds (U) and allocate them for growth (the fraction eU, with e denoting the microbial growth efficiency), enzyme production (E_P), and synthesis of osmolytes (Π). Respiration associated to growth ($R_G = (1-e)U$) and maintenance (R_M) are also accounted for (as described below, respiration associated to enzyme production is already included in the growth efficiency). We neglect instead C allocation to extracellular compounds other than enzymes (e.g., extra-cellular polysaccharides). Exchanges between active (subscript A) and dormant biomass (subscript D) are denoted by $P_{D\to A}$ and $P_{A\to D}$. The transition to dormancy may be enhanced by lack of substrates to synthesize osmolytes, so that in some conditions $P_{A\to D}$ is increased by a factor $\varphi > 1$ (Section 2.3.1). Active and the dormant biomass also decay due to mortality (M_B, $M_{B,D}$), feeding the soluble organic matter compartment. Osmolytes released upon rewetting ($P_{D\to A}C_{O,D}/C_{B,D}$) and associated to mortality of both active and dormant populations are also returned to the C_D pool. Enzyme and soluble organic C may also be lost through leaching (respectively L_E and L_D). With reference to Fig. 1, the mass balance equations of the C pools can be written as,

$$\frac{dC_S}{dt} = I_L(t) - D, \tag{1}$$

$$\frac{dC_D}{dt} = D + M_B\left(1 + \frac{C_O}{C_B}\right) + M_{B,D}\left(1 + \frac{C_{O,D}}{C_{B,D}}\right) + E_D + P_{D\to A}\frac{C_{O,D}}{C_{B,D}} - U - L_D, \tag{2}$$

$$\frac{dC_E}{dt} = E_P - E_D - L_E, \tag{3}$$

$$\frac{dC_B}{dt} = U - R_G - R_M - E_P - \Pi + P_{D\to A} - \varphi P_{A\to D} - M_B, \tag{4}$$

$$\frac{dC_{B,D}}{dt} = \varphi P_{A\to D} - P_{D\to A} - M_{B,D}, \tag{5}$$

$$\frac{dC_O}{dt} = \Pi - (P_{A\to D} + M_B)\frac{C_O}{C_B}, \tag{6}$$

Table 2
List of time-invariant parameters and their values.

Symbol	Description	Value	Units	Sources and notes
a_1	Mass of water per unit dry mass of biomass	1.4	g g^{-1}	(Potts, 1994; Dotsch et al., 2008)
a_2	Mass of C per unit dry mass of biomass	0.5	gC g^{-1}	(Bratbak and Dundas, 1984; Loferer-Krossbacher et al., 1998)
a_3	Molecular weight of a representative osmolyte	60	g mol^{-1}	For glutamate or proline
a_4	Dry weight per cell	10^{-13}	g cell^{-1}	(Loferer-Krossbacher et al., 1998)
b	Exponent of the water retention curve	4.9	–	(Rodriguez-Iturbe and Porporato, 2004)
$c_{A\to D}$	Osmolyte concentration at half the rate $k_{A\leftrightarrow D}$	0.01–0.2	gC gC^{-1}	Assumed range[a]
$C_{D,0}$	Soluble organic C concentration outside the microbial cell	0	gC m^{-3}	Assumed
$C_{E,0}$	Enzyme concentration outside the microbial cell	2–10	gC m^{-3}	Assumed range[a]
$D_{D,0}$	Diffusivity of dissolved organic C in pure water	8.1×10^{-10}	m^2 s^{-1}	For amino acids, after Jones et al. (2005)
$D_{E,0}$	Diffusivity of enzymes in pure water	$D_{D,0}/10$	m^2 s^{-1}	(Vetter et al., 1998)
e	Growth efficiency	0.5	–	(Schimel and Weintraub, 2003)
$k_{A\leftrightarrow D}$	Maximum rate of transition between microbial activity states	1	d^{-1}	Assumed
$k_{A\to D}$	Maximum rate of transition from active to dormant state	$k_{A\leftrightarrow D}$	d^{-1}	Assumed
k_B	Mortality rate of active population	0.012	d^{-1}	(Schimel and Weintraub, 2003)
$k_{B,D}$	Mortality rate of dormant population	$k_B/10$	d^{-1}	(Bär et al., 2002)
k_D	Maximum rate of decomposition	10^{-3}	m^3 gC^{-1} d^{-1}	Derived from Schimel and Weintraub (2003)
$k_{D\to A}$	Maximum rate of transition from dormant to active state	$k_{A\leftrightarrow D}$	d^{-1}	Assumed
K_d	Solid-liquid partition coefficient	10^{-5}	m^3 g^{-1}	(Raab et al., 1999)
k_E	Enzyme de-activation rate	0.05	d^{-1}	(Schimel and Weintraub, 2003)
k_M	Maintenance respiration rate	0.022	d^{-1}	(Schimel and Weintraub, 2003)
k_{sat}	Soil hydraulic conductivity at saturation	0.8	m d^{-1}	(Rodriguez-Iturbe and Porporato, 2004)
m_1	Empirical exponent	1.5	–	(Hamamoto et al., 2010)
m_2	Empirical exponent	2.5	–	(Hamamoto et al., 2010)
n	Soil porosity	0.43	–	(Rodriguez-Iturbe and Porporato, 2004)
R	Gas constant	8.314	J mol^{-1} K^{-1}	
s_{th}	Diffusion threshold	0.18	–	Assumed equal to the plant wiling point
T	Temperature	298	K	Assumed
Z_r	Soil depth	0.4	m	Assumed
χ	Parameter group, $\chi = a_1 a_3/(a_2 \rho_w RT)$	0.067	MPa^{-1}	Calculated
γ	C_O/C_B ratio for constitutive osmolyte production	0.026	–	(Boot et al., 2013)
δ	Characteristic distance between microbial cells and substrate	10^{-5} to 10^{-3}	m	Assumed range[a]
ν	Scaling coefficient, $\nu \approx \delta A/V$	6	–	Calculated
π_B	Microbial turgor pressure	0.1	MPa	(Potts, 1994)
ρ_b	Soil bulk density	1.2×10^6	g m^{-3}	Assumed
ρ_w	Density of liquid water	10^6	g m^{-3}	
$\psi_{A\to D}$	Water potential at 50% of the maximum rate $k_{A\to D}$	$\pi_B - c_{A\to D}/\chi$	MPa	For inducible osmolytes: calculated as a function of $c_{A\to D}$
		$-\gamma/\chi = -0.4$	MPa	For constitutive osmolytes: calculated at $\pi_B = 0$
$\psi_{D\to A}$	Water potential at 50% of the maximum rate $k_{D\to A}$	$\psi_{A\to D}/4$	MPa	Assumed
ψ_{sat}	Soil water potential at saturation	−0.002	MPa	(Rodriguez-Iturbe and Porporato, 2004)
ω	Sensitivity parameter for the switching functions	4	–	Assumed

[a] Asterisks indicate parameters varied in the sensitivity analyses.

$$\frac{dC_{O,D}}{dt} = P_{A\to D}\frac{C_O}{C_B} - (P_{D\to A} + M_{B,D})\frac{C_{O,D}}{C_{B,D}}, \quad (7)$$

The full explanation of these equations and the mathematical representations of the C fluxes are described in the following sections.

2.2. Microbial metabolism

The decomposition flux is defined following Schimel and Weintraub (2003),

$$D(C_S, C_E) = k_D C_S C_E, \quad (8)$$

where k_D is the maximum rate of decomposition. Substrate uptake by microbes is described as a mass transfer process mediated by soil moisture,

$$U(C_D) = h_D(s)(C_D - C_{D,0}) \approx h_D(s) C_D, \quad (9)$$

where h_D is a mass transfer function accounting for diffusion limitations in the delivery of dissolved compounds to microbes (Section 2.5), and $C_{D,0}$ the substrate concentration at the cell surface, assumed here to be much smaller than in the bulk soil. Equation (9) assumes that C uptake is solely controlled by its availability and not by the amount of active biomass. This approximation holds when either a fraction of active biomass is always present, or when the recovery from dormancy is sufficiently fast to restore an active population. It is also possible that microbial groups exhibit different responses to the available dissolved substrates, resulting in a community-level uptake rate that differs from the highly idealized Equation (9), possibly depending also on C_B (Ågren and Wetterstedt, 2007).

Enzyme activity tends to decline in dry conditions (Toberman et al., 2008; Steinweg et al., 2012). However, this decline is slower than that of solute diffusivity and microbial activity, so that the function D is assumed to be independent of soil moisture. Microbial mortality and enzyme deactivation are described as first order rate processes (Schimel and Weintraub, 2003), with kinetic constants denoted by k_B, $k_{B,D}$, and k_E. Also, the dormant population is assumed to decay slower than the active population, so that $k_B > k_{B,D}$ (Bär et al., 2002). As a consequence, depending on the climatic conditions that trigger dormancy and the difference between the mortality rates of the two populations, the model is able to reproduce scenarios ranging from no dormant biomass (favorable moisture and relatively high $k_{B,D}$) to a large dormant fraction of the population (frequently dry or C-poor soils and low $k_{B,D}$). In Equations (6) and (7), the last terms on the right hand side represent the osmolyte transfer to the pool of dissolved C associated to mortality from both active and dormant populations. The fate of excess osmolytes after rewetting is still debated (e.g., see Halverson et al., 2000; Tiemann and Billings, 2012). Here, it is assumed that after rewetting, osmolytes in excess are released from the dormant biomass to the environment (i.e., the term $P_{D\to A}C_{O,D}/C_{B,D}$ in Equation (2)), whereas excess osmolytes in the active biomass are metabolized. When osmolytes are metabolized due to increased water potential, the flux Π in Equations (4) and (6) turns negative (Section 2.3.1).

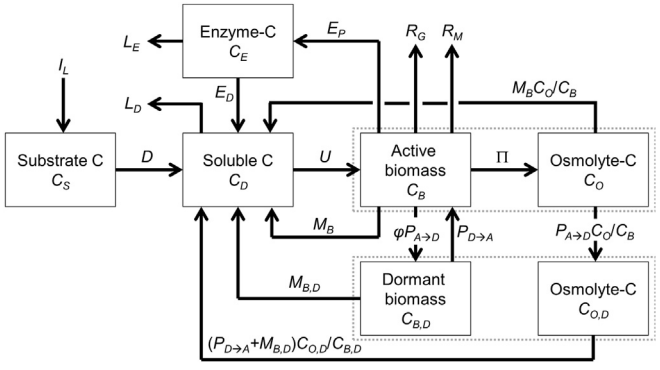

Fig. 1. Model scheme: boxes represent carbon compartments and arrows indicate fluxes (the direction of the arrow is consistent with the sign convention used in the equations). Dashed boxes highlight the association between the biomass and osmolyte pools; symbols are defined in Table 1.

The respiration formulation deviates from the one in Schimel and Weintraub (2003). Here, a constant fraction of the C taken up (U) is assumed to be respired to build biomass or intra-cellular compounds ($R_G = (1 - e)U$). As a result, the net input of C into the microbial biomass is given by eU. From this input, maintenance respiration ($R_M = k_M C_B$) and C used for enzyme and osmolyte synthesis are subtracted. No specific respiration terms are associated with enzyme and osmolyte synthesis because they are already accounted for in the growth efficiency e.

The enzyme pool receives an input E_P from the microbial biomass. Assuming that enzymes diffuse in the soil like soluble organic C (albeit with a different diffusivity, see Section 2.5), in analogy to Equation (9) we can write,

$$E_P(C_E) = h_E(s)(C_{E,0} - C_E), \quad (10)$$

where the enzyme concentration at the microbial cell surface, $C_{E,0}$, is fixed. When enzyme concentration increases or when soil moisture decreases, thus reducing h_E, Equation (10) predicts lower enzyme production. In this way, C investment in enzymes is regulated based on demand (linked to the dynamics of C_E), delivery efficiency (mediated by h_E), and biological strategies, which set the value of $C_{E,0}$. Equation (10) implies that enzyme synthesis is uncoupled from growth; however, both enzyme synthesis and growth depend on diffusivity (through h_D and h_E), so that E_P remains low when substrate availability is limiting growth in dry conditions.

Osmolyte production (Π) is defined so that the concentration of osmolytes in the microbial cells balances changes in soil water potential (Section 2.3). The exchange of biomass between active and dormant compartments ($P_{D\to A}$ and $P_{A\to D}$) is described in Section 2.4. Osmolytes associated with active biomass that becomes dormant accumulate in the $C_{O,D}$ pool (at a rate $P_{A\to D}C_O/C_B$), from which they are returned to the soluble organic matter compartment when the dormant microbial biomass is reactivated (at a rate $P_{D\to A}C_{O,D}/C_{B,D}$).

2.3. Osmoregulation

Two osmoregulation strategies are implemented: i) inducible osmolyte synthesis that allows maintaining a stable turgor pressure (Section 2.3.1) and ii) constitutive osmolyte synthesis, in which a constant osmolyte concentration is maintained, while turgor pressure fluctuates following changes in soil water potential (Section 2.3.2).

2.3.1. Inducible osmolyte production

Microbes are assumed to maintain a stable turgor pressure (π_B) by altering the osmotic potential of the cells (Ω_B) as soil matric potential (ψ) changes. Thermodynamic equilibrium is assumed for simplicity so that the matric potential is matched by the sum of turgor pressure and osmotic potential, $\psi = \pi_B + \Omega_B$. Hence, for a set value of π_B, microbial osmoregulation has to vary Ω_B as soil

moisture varies. Following Van't Hoff relation, the osmotic potential can be related to the concentration of intra-cellular osmolytes (Griffin, 1981; Dotsch et al., 2008),

$$\Omega_B = \psi - \pi_B = -RT\sum_i c_i \approx -RTc, \tag{11}$$

where $R = 8.314$ J mol^{-1} K^{-1}, T is the temperature (K), and c_i is the concentration of each osmolyte in the cytoplasm free water (mol m^{-3}). For simplicity, a single representative compound is considered (with concentration c), and changes in microbial cell volume are neglected. Accordingly, c can be converted from a molar concentration to a concentration of osmolyte C per unit microbial C,

$$\frac{C_O}{C_B} = c\frac{a_1 a_3}{a_2 \rho_w}, \tag{12}$$

where a_1 is the mass of water per unit dry mass of biomass, a_2 is the mass of C per unit dry mass of biomass, a_3 is the molecular weight of a representative osmolyte, and ρ_w is the density of liquid water. Assuming that microbial cells are composed of roughly 70% water (Potts, 1994), but that only 60% of that is 'free' (not bound) cytoplasmic water available as a solvent for osmolytes (Dotsch et al., 2008), a_1 can be estimated as about 1.4 g of water per g of biomass dry weight. Parameter a_2 is set to 0.5 gC per g of biomass dry weight (Bratbak and Dundas, 1984; Loferer-Krossbacher et al., 1998) and $a_3 = 60$, assuming that a representative osmolyte molecule contains five C atoms, each with molecular weight of 12 gC mol^{-1} (e.g., glutamate, proline, see Williams and Xia, 2009; Boot et al., 2013). Inorganic solutes can also be used as osmolytes, but only in response to extreme water potential values (Killham and Firestone, 1984), at which the transition to dormancy is assumed to have already occurred. Accordingly, this contribution is neglected and the formulation only accounts for organic osmolytes. We also note that Eq. (12) assumes that solutes are diluted and their contribution to the value of a_1 is neglected.

Combining Equations (11) and (12), the expression linking osmolyte concentration (per unit biomass C) to soil water potential is found as,

$$\frac{C_O}{C_B} = \frac{a_1 a_3}{a_2 \rho_w}\frac{\pi_B - \psi}{RT} = \chi(\pi_B - \psi), \tag{13}$$

where all the constant parameters are grouped in the coefficient $\chi = a_1 a_3/(a_2 \rho_w RT)$. Microbial turgor pressure π_B is assumed constant and equal to 0.1 MPa (Potts, 1994). Based on the parameter values reported above and at $T = 25$ °C, $\chi = 0.067$, indicating that when $\psi = -1$ MPa about 6% of microbial biomass C is constituted of osmolytes. Using $\chi = 0.067$, Equation (13) predicts well the nearly linear scaling between cytoplasmic C concentration and water potential observed up to about −8 MPa in experiments with controlled salinity (Killham and Firestone, 1984; Schimel et al., 1989) (Fig. 2). Equation (13) implies instantaneous osmoregulation, which is a reasonable assumption at the daily time scale considered here, since both accumulation and release of osmolytes occur at much shorter time scales (Kayingo et al., 2001; Dotsch et al., 2008).

The concentration of osmolytes per unit microbial C is constrained to be only a function of soil water potential by specifying the flux Π in Equations (4) and (6). This constraint also implies that the two mass balance equations for C_B and C_O can be reduced to a single differential equation in addition to Equation (13). Π can be computed by noting from Equation (13) that

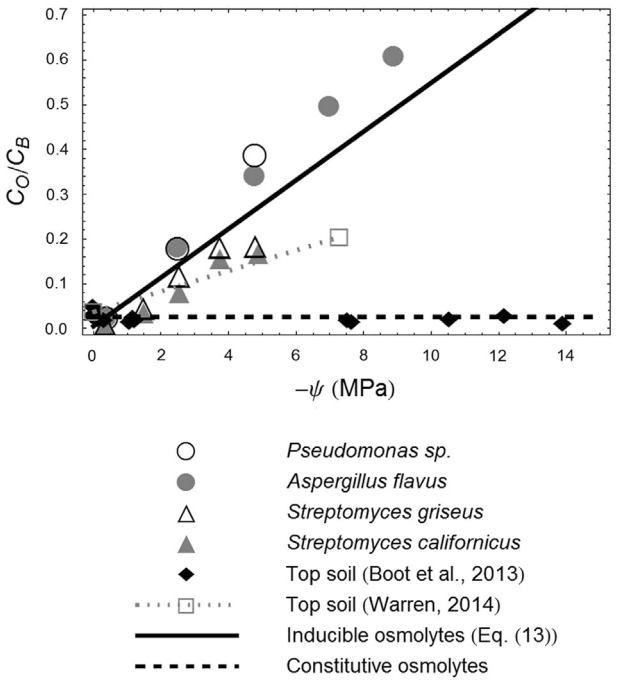

Fig. 2. Ratio of osmolyte C to microbial C (C_O/C_B) as a function of water potential (ψ), for two contrasting response strategies: inducible osmolyte production (solid line, circles and triangles) and constitutive osmolyte production (dashed line, filled diamonds). Organisms showing inducible osmolyte production were subject to salt stress (data for *Pseudomonas* and *Aspergillus* are from Schimel et al. (1989); data for the *Streptomyces* species are from Killham and Firestone (1984)); the solid line is from Equation (13), with $\chi = 0.067$, without any parameter adjustment. Organisms with constant osmolyte concentration were sampled under field conditions (Boot et al., 2013); the dashed line represents the mean C_O/C_B for this soil community. Data from a different soil showing a mixed response are also shown (open squares, Warren, 2014); ψ in this study was estimated using a water retention curve with $b = 5$ and ψ_{sat} back-calculated from the reported soil moisture at field capacity; biomass C was obtained from chloroform-labile C without further corrections.

$$\frac{dC_O}{dt} = \frac{d}{dt}[\chi(\pi_B - \psi)C_B] = -\chi C_B\frac{d\psi}{dt} + \chi(\pi_B - \psi)\frac{dC_B}{dt}, \tag{14}$$

where the first term on the right hand side describes changes in C_O due to variations in water potential, and the second term accounts for dilution of osmolytes in the growing (or decreasing) biomass. Using Equations (6) and (14), Π can thus be found as

$$\Pi = -\chi C_B\frac{d\psi}{dt} + \chi(\pi_B - \psi)\frac{dC_B}{dt} + P_{A\to D}\frac{C_O}{C_B} + M_B\frac{C_O}{C_B}. \tag{15}$$

Substituting this expression for Π into Equation (4), the differential dC_B/dt can be rewritten as,

$$\frac{dC_B}{dt} = \frac{eU - R_M - E_P + P_{D\to A} + \chi C_B\frac{d\psi}{dt}}{1 + \chi(\pi_B - \psi)} - \varphi P_{A\to D} - M_B, \tag{16}$$

where the term $\varphi P_{A\to D}$ refers to microbes becoming dormant. When there are sufficient C resources to match the demand set by Π, $\varphi = 1$; otherwise, $\varphi > 1$ and the transition to dormancy is accelerated (Equation (17)). By constraining the osmolyte concentration in the active biomass, Equation (16) substitutes Equations (4) and (6) in the original system of differential equations.

When solute diffusivity declines, the microbial biomass cannot be supplied with enough soluble organic C to meet the demand for osmolyte production, set by Π (Equation (15)). Under these conditions, it is assumed that Π is limited by the rate of C assimilation,

eU, and the rate of transition to the dormant state increases by a factor φ (note that this increase is de-coupled from the transfer of osmolytes from the active to the dormant population). For Equation (13) to still hold, it can be shown that

$$\varphi = \begin{cases} 1 - \frac{1}{P_{A\to D}}\left[\frac{eU+\chi C_B \frac{d\psi}{dt}}{\chi(\pi_B-\psi)} + P_{D\to A} - R_M - E_P\right] & \Pi \geq eU \\ 1 & \Pi < eU \end{cases}. \quad (17)$$

Accordingly, when all assimilated C is used for osmoregulation, the mass balance equation for the active microbial biomass becomes (from Equation (4) by imposing $\Pi = eU$),

$$\frac{dC_B}{dt} = -R_M - E_P + P_{D\to A} - \varphi P_{A\to D} - M_B. \quad (18)$$

2.3.2. Constitutive osmolyte production

When constitutive osmolytes are employed, microbes maintain a fixed concentration of osmolytes in both active and dormant biomass, i.e., $C_O/C_B = C_{O,D}/C_{B,D} = \gamma$. Assuming a constant osmolyte concentration implies no active osmoregulation as the soil water potential changes. As a consequence, turgor pressure decreases with soil moisture, eventually reaching zero. We assume that dormancy is triggered by this decrease in turgor pressure, so that microbes remain active as long as their turgor is positive (see Section 2.6 for details).

Because osmolyte concentrations are proportional to C_B and $C_{B,D}$, Equations (6) and (7) become redundant. Moreover, we neglect supply limitations ($\varphi = 1$), because osmolyte synthesis decreases as microbial growth slows down during dry periods, unlike the case of inducible osmolytes. Based on these assumptions, the mass balance equation for the active microbial biomass can be written as,

$$\frac{dC_B}{dt} = \frac{eU - R_M - E_P + P_{D\to A}}{1+\gamma} - P_{A\to D} - M_B. \quad (19)$$

2.4. Dormancy and reactivation

The active microbial biomass is assumed to switch to a dormant state as the osmolyte concentration increases when inducible osmolytes are used, or as turgor pressure drops to zero when constitutive osmolytes are used. In the former case, the switch to dormant state can be equally modeled as a function of osmolyte concentration or ψ, because internal osmolytes are regulated as a function of soil water potential through Equation (13). In the latter case of constitutive osmolytes, the trigger is π_B, which is also linked to ψ when osmolyte concentration is fixed. In both cases, the rates of transfer between active and dormant biomass are described as first order rate processes (Bär et al., 2002; Jones and Lennon, 2010; Stolpovsky et al., 2011), where the rate depends nonlinearly on ψ,

$$P_{A\to D}(C_B) = k_{A\to D} f_{A\to D}(\psi) C_B, \quad (20)$$

$$P_{D\to A}(C_{B,D}) = k_{D\to A} f_{D\to A}(\psi) C_{B,D}, \quad (21)$$

where $k_{A\to D}$ and $k_{D\to A}$ are the maximum rates of transition and $f_{A\to D}$ and $f_{D\to A}$ are the switching functions linking the rate of transition to the environmental conditions. Various mathematical expressions have been proposed for these functions (Bär et al., 2002; Jones and Lennon, 2010; Stolpovsky et al., 2011), but they all have similar sigmoidal shape rising from 0 where no transitions occur to 1 where the maximum rate is achieved. For simplicity, we selected a rational function (Fig. 3A),

$$f_{A\to D}(\psi) = \frac{(-\psi)^\omega}{(-\psi)^\omega + (-\psi_{A\to D})^\omega}, \quad (22)$$

which equals 0 at $\psi = 0$, indicating that active biomass in well-watered condition does not switch to a dormant state, increases to 1/2 at $\psi = \psi_{A\to D}$, and eventually approaches 1 as ψ becomes more negative, indicating that in dry soils the maximum rate of transition to the dormant state is achieved. Using Equation (13), the value of $\psi_{A\to D}$ can be related to a concentration of osmolytes or turgor pressure, thus giving this parameter a specific physiological meaning. The exponent ω represents the steepness of the curve around $\psi_{A\to D}$, with larger values causing a more abrupt transition. The transition back to the active state follows a relation decreasing from 1 to 0 as the soil becomes drier,

$$f_{D\to A}(\psi) = \frac{(-\psi_{D\to A})^\omega}{(-\psi)^\omega + (-\psi_{D\to A})^\omega}. \quad (23)$$

where the water potential at 50% of the maximum rate ($\psi_{D\to A}$) is less negative than the one in Equation (22). This difference causes a hysteretic behavior capturing a delay in the response upon rewetting. The actual time delay depends on the speed of the rewetting

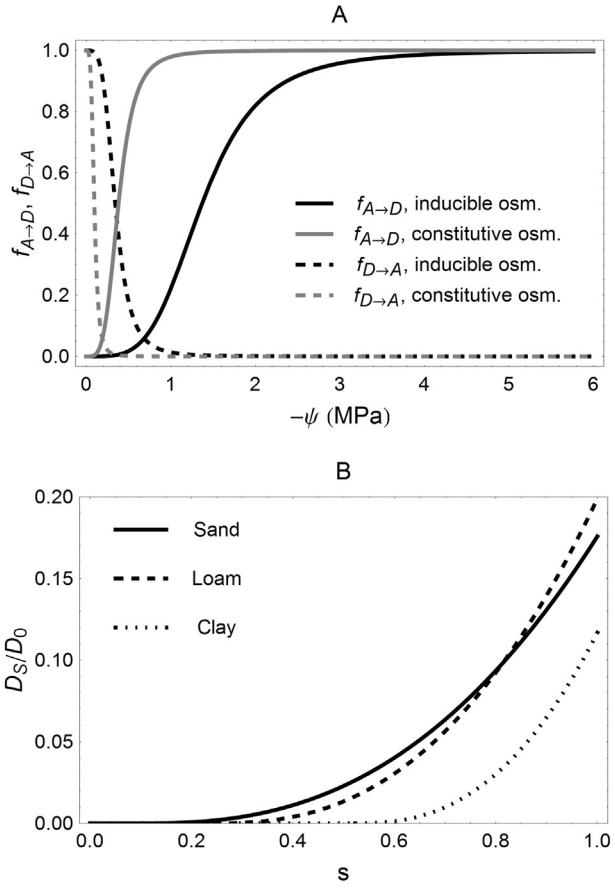

Fig. 3. A) Normalized transition rates between active and dormant biomass ($f_{A\to D}$) and vice versa ($f_{D\to A}$), as a function of soil water potential (ψ), for inducible (black curves) and constitutive (gray) osmolyte production (Equations (22) and (23), with $\psi_{D\to A} = \psi_{A\to D}/4$, $\omega = 4$). B) Effect of relative volumetric soil moisture (s) on solute diffusivity (D_S/D_0, Equation (24)), for three soil types (hydraulic parameters are from Rodriguez-Iturbe and Porporato (2004)).

and becomes negligible when rewetting is rapid and sufficiently intense to increase water potential to values close to zero (above the soil field capacity).

For simplicity, the maximum rates of transition are assumed equal, denoting them by $k_{A\leftrightarrow D}$. Also, mortality upon rewetting is neglected, as microbes can release osmolytes rapidly (with respect to the daily time scale) when conditions change (Kayingo et al., 2001), leading to little cell lysis (Fierer and Schimel, 2003). The four parameters $k_{A\leftrightarrow D}$, $\psi_{A\to D}$, $\psi_{D\to A}$, and ω in Equations (20)–(22) represent specific eco-physiological traits that determine the drought response strategy of the microbial community. Importantly, the values of $\psi_{A\to D}$ and $\psi_{D\to A}$ depend on the osmolyte synthesis strategy, as described in Section 2.6.

2.5. Diffusion of dissolved organic C and enzymes

As soil moisture decreases, the water-filled pores become smaller and eventually disconnected, thus decreasing the effective solute diffusivity in the soil (D_S), which in turn affects the transfer of solutes to the microbial cells. The dependence of solute diffusivity on soil moisture is described by the empirical function (Moldrup et al., 2001; Olesen et al., 2001b; Hamamoto et al., 2010) (Fig. 3B),

$$\frac{D_D(s)}{D_{D,0}} = n^{m_1}(1-s_{th})^{m_1}\left(\frac{s-s_{th}}{1-s_{th}}\right)^{m_2}, \tag{24}$$

where s_{th} the percolation threshold for solute diffusion (assumed equal to the soil moisture at the plant wilting point for simplicity), m_1 and m_2 are two empirical exponents (about 1.5 and 2.5, respectively), and $D_{D,0}$ is the diffusivity of the solute in pure water.

Using Equation (24) and setting geometric constraints on the location of microbial cells or colonies with respect to their substrates, it is possible to compute the mass transfer function h_D (Equation (9)),

$$h_D(s) \approx \frac{1}{ns+\rho_b K_d}\frac{D_D(s)}{\delta}\frac{A}{V} = \frac{\nu}{ns+\rho_b K_d}\frac{D_D(s)}{\delta^2}, \tag{25}$$

where δ is a characteristic distance between microbes and substrate, A is the area around the microbial colony crossed by the diffusing substrates, V the volume of soil affecting that colony, K_d is the solid–liquid partition coefficient ($m^3\ g^{-1}$), and ρ_b is the soil bulk density. The term $ns + \rho_b K_d$ takes into account sorption and converts C_D (g m^{-3} of soil) to a concentration in the liquid phase (Olesen et al., 2001a). As a first approximation, the ratio A/V is assumed to be approximated by ν/δ, where the scaling coefficient ν depends on the specific geometry of the soil system. For a spherical or cubical volume around the microbial cells, $\nu = 6$. Analogous derivations lead to the transfer coefficient for enzyme diffusion from the microbial cells to the site of reaction, except that the enzyme diffusivity in pure water ($D_{E,0}$) is about 1/10 of the diffusivity for dissolved organic substrates due to their larger molecular weight (Vetter et al., 1998).

2.6. Model parameterization and simulation scenarios

Most model parameters are obtained from published sources (Table 2). In particular, biogeochemical rates and microbial growth efficiency are taken from Schimel and Weintraub (2003) and hydrologic parameters for a sandy loam soil from Rodriguez-Iturbe and Porporato (2004, Table 2.1). The chosen parameters are not meant to describe a specific ecosystem, but to provide a generic parameterization for processes that are not studied in the sensitivity analyses. A sub-set of eco-physiological parameters could not be determined based on previous studies: four parameters encoding the dormancy/reactivation process ($k_{A\leftrightarrow D}$, $\psi_{A\to D}$, $\psi_{D\to A}$, and ω) and one describing C investment to enzyme production ($C_{E,0}$). To reduce the number of parameters in the sensitivity analyses, we set $\omega = 4$ and $k_{A\leftrightarrow D} = 1\ d^{-1}$, on the grounds that transition to dormant state and re-activation generally follow rapidly the changes in environmental conditions (Oliver, 2005). We also imposed the constraint that water potential at 50% transition rate to active status ($\psi_{D\to A}$) equals 1/4 of the threshold for transition to dormant status ($\psi_{A\to D}$), to capture a lagged transition back to active status upon rewetting.

The value of $\psi_{A\to D}$ is determined in different ways, depending on the osmolyte synthesis strategy (inducible *vs.* constitutive). For inducible osmolytes, $\psi_{A\to D}$ is expressed using Equation (13) as a function of a threshold osmolyte concentration in the microbial cell ($c_{A\to D}$), $\psi_{A\to D}=\pi_B-c_{A\to D}/\chi$. This representation provides a link between the rate of transition to dormancy and a possible physiological transition trigger. For constitutive osmolytes, we assumed that the transition to dormancy occurs when turgor pressure reaches zero. Because microbial cells could exhibit different turgor pressures, a distribution of π_B occurs at the community level. As a consequence, the community-level transition to dormancy follows a sigmoidal curve with $\psi_{A\to D}$ corresponding to the water potential at which the average π_B reaches zero. Rearranging Equations (11) and (13) for $\pi_B = 0$, this water potential is found as $\psi_{A\to D} = -(C_O/C_B)\chi^{-1}$. The average value of C_O/C_B (based on glutamate C) in a soil microbial community that exhibits little osmoregulation over a wide range of water potentials was 0.026 (Boot et al., 2013; see Fig. 2). We use this value, together with the estimated $\chi = 0.067$, to obtain $\psi_{A\to D} = -0.4$ MPa.

The characteristic distance, δ, could not be reliably estimated based on available data. Hence, it is here treated as an empirical parameter ranging from a minimum value of 10^{-5} m to a maximum value of 10^{-3} m (see Appendix B for details on the estimation of these bounds). We are not aware of any studies measuring enzyme concentrations around the microbial cells and thus assume that $C_{E,0}$ is about one order of magnitude smaller than the biomass C. With this assumption, the enzyme synthesis rate strongly depends on environmental conditions: for a set $C_{E,0}$, higher moisture levels favor enzyme diffusion and hence tend to increase the rate of enzyme synthesis (Equation (10)).

To summarize, we set the values of parameters for which empirical information is available, and perform sensitivity analysis on the three remaining most uncertain parameters: $c_{A\to D}$, $C_{E,0}$, and δ. We also compared the effect of inducible *vs.* constitutive osmolyte synthesis for each set of parameters. Sensitivity analysis were performed by illustrating how C fluxes and pools change when altering the values of these critical parameters and by calculating the elasticity of heterotrophic respiration to changes in the parameter values. Elasticity is a non-dimensional measure of sensitivity defined for a flux F affected by a generic parameter a as

$$E_a = \frac{\partial F}{\partial a}\frac{a}{F}. \tag{26}$$

In our case F indicates respiration, which is affected by model parameters indirectly, through changes in the temporal trajectories of the C pools. Therefore, the elasticity is estimated numerically by means of a finite difference approach and through time, based on a set of simulations with the same initial condition, but different values of the parameter of interest (baseline − 10%, baseline, baseline + 10%).

Two sets of analyses were performed: at steady state and during transient changes in soil moisture. The steady state of the system is analytically calculated by imposing that all the time derivatives in Equations (1)–(7) are zero. Soil moisture is in this case treated as an

external parameter to be varied according to climatic conditions. For this analysis, we assumed that the litterfall input declines as the long-term soil moisture decreases, consistent with declining plant productivity along a precipitation gradient. Litterfall I_L is assumed to be proportional to the rate of evapotranspiration (Appendix A), declining from a maximum rate of 10 gC m^{-3} d^{-1} under well watered conditions to zero at the plant wilting point. Steady state pools are thus represented as a function of soil moisture and the other eco-physiological parameters. Second, we consider changes of soil moisture through time and investigate the dynamic response of the C compartments. For these simulations, we assumed initial conditions equal to the steady state solution at an intermediate value of $s = 0.6$, at which microbial activity is not limited by oxygen (not modeled here) or water availability.

3. Results

3.1. Steady state analysis

The model was first used to assess the partitioning of C among the different compartments under equilibrium conditions, that is, in the long-term at a given soil moisture. To allow a visual comparison among C pools varying by several orders of magnitude, Fig. 4 shows the cumulative C fractions on a logarithmic scale: each shaded area represents the C fraction in a specific compartment, with blank areas indicating substrate C. Also, water potential is used instead of volumetric soil moisture to highlight patterns in the dryer end of the moisture gradient. In general, moister conditions favor microbial growth and hence the fractions of active microbial biomass and enzyme C are larger. Moving towards drier conditions, osmolytes accumulate and part of the microbial biomass turns dormant. In very dry conditions, the dormant biomass becomes predominant and osmolyte concentrations decline (as a fraction of total soil C), as microbes switch from osmoregulation to dormancy. In these dry conditions, solute diffusivity is low and hence soluble organic C may accumulate relative to the other pools.

These patterns depend strongly on microbial strategies to cope with water stress. Increasing investment in enzymes (larger $C_{E,0}$) may increase the pool of soluble organic C, thus partly overcoming diffusion limitations as soils dry. As a consequence, larger $C_{E,0}$ favors the transfer of C from SOM to the microbial pools at any soil moisture level (compare Fig. 4A with Fig. 4C). In contrast, producing

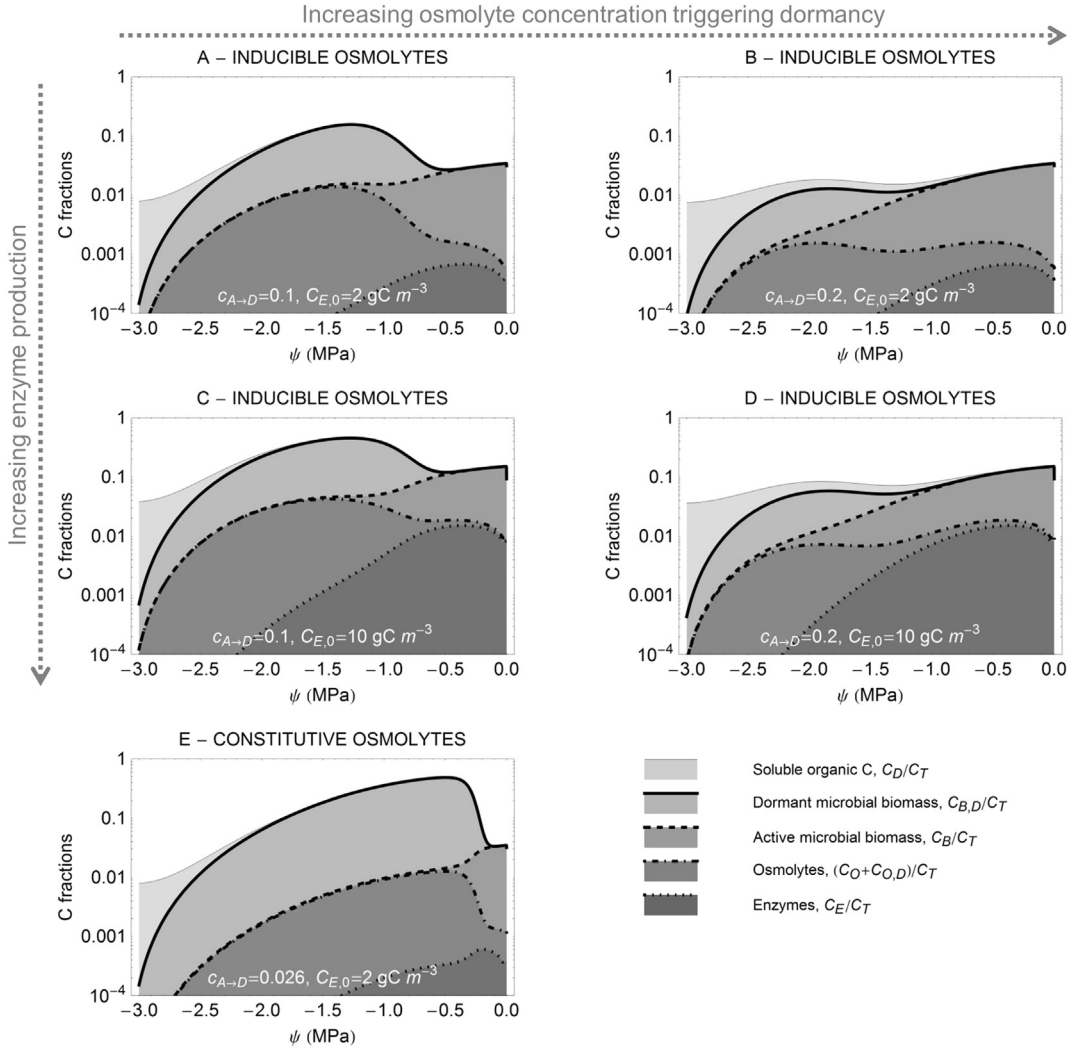

Fig. 4. Steady state partitioning of soil C into the main modeled pools, for inducible (A to D) or constitutive osmolyte production (E). In the case of inducible osmolytes, different values of the threshold osmolyte concentration ($c_{A\to D}$, increasing from left to right as indicated by the horizontal arrow) and enzyme concentration around the microbial cell ($C_{E,0}$, increasing from top to middle panels following the vertical arrow) are considered. Enzyme C (C_E), osmolyte C ($C_O + C_{O,D}$), active and dormant biomass (respectively C_B and $C_{B,D}$), and soluble C (C_S) are represented on a fractional basis with respect to the total C stored at steady state in the soil (blank areas represent C_S).

larger osmolyte concentrations before becoming dormant (larger $c_{A\to D}$) allows microbes to remain active at lower soil moisture (compare Fig. 4A with Fig. 4B). However, larger $c_{A\to D}$ lowers the overall biomass C compared to the case of low $c_{A\to D}$. As a result, the osmolyte amounts necessary to sustain this smaller biomass pool is also reduced. Microbes that maintain a fixed osmolyte concentration will become dormant earlier than microbes employing inducible osmolytes, because they have lower $c_{A\to D}$ (Fig. 4E). Hence, the steady state dormant biomass pool for microbes with constitutive osmolytes extends to less negative water potentials than in the case of inducible osmolytes.

3.2. Temporal dynamics during dry/wet cycles

Figs. 5 and 6 illustrate the temporal evolution of the C compartments and fluxes, respectively, during two drying periods interspaced by a rainfall event that restores well-watered conditions (Fig. 5A). The different colors of the curves indicate inducible (black) and constitutive (gray) osmolyte synthesis. As the soil dries, three phases characterizing microbial metabolism can be recognized: i) stable microbial phase in well-watered conditions, ii) active osmoregulation in response to changes in soil water potential (only for inducible osmolytes), and iii) transition to dormant state as the threshold osmolyte concentration in the cell is reached. Fig. 5C shows the decline of the active biomass pool as the osmolyte concentration (Fig. 5D) reaches the threshold $c_{A\to D}$, at which the rate of transition to dormancy is half of the maximum rate. As a result, the dormant population and its own osmolyte pool increase until they stabilize when the whole population has become dormant. As these physiological changes occur, the rate of substrate supply declines due to decreasing solute diffusivity (Fig. 6A). As a result, soluble organic C increases because enzyme activity is not inhibited by low moisture values (Fig. 5B). Upon rewetting, large amounts of dissolved C become suddenly available and can be taken up by the reactivated microbial population, resulting in a respiration pulse. Because this pulse of activity rapidly depletes the DOC pool, microbial growth quickly stabilizes, until water availability changes again. During rewetting, osmolytes associated to the dormant population are recycled as dissolved C, and osmolytes associated to the active population are converted to new biomass (negative Π in Fig. 6D).

Microbes with inducible (black curves) and constitutive (gray) osmolytes share the main features of these patterns. However, microbes with constitutive osmolytes turn to a dormant state earlier during the soil drying, resulting in earlier peaks of dormant biomass and active to dormant biomass transition rates. The shorter active period in microbes using constitutive osmolytes causes lower enzyme production and therefore slightly lowers accumulation of soluble substrates (Fig. 5B). However, lower maintenance respiration during the dry period counters the lower substrate availability (Fig. 6B), making the overall C balance of the two osmoregulation modes comparable.

Soil moisture effects on C fluxes during a prolonged drying event are shown in Fig. 7, for different values of the eco-physiological parameters $c_{A\to D}$ and $C_{E,0}$, and at two different distances between substrates and microbes, δ. As soil moisture decreases, substrate supply to the microbes (and to a lesser extent also the decomposition rate) declines, as also noted in Fig. 6. As a consequence, respiration declines too. Dry conditions first trigger osmoregulation (Fig. 7D) and later dormancy as soil moisture declines (Fig. 7E). Moreover, the decreased enzyme diffusion rate as soil dries lowers C allocation to enzyme production (Equation (10); see Fig. 7B). Allocating more resources to enzymes (larger $C_{E,0}$) would improve uptake rates, but would not alter the soil moisture level at which respiration stops (not shown). In contrast, switching to dormancy at higher $c_{A\to D}$ may delay the reduction of respiration, because microbes become dormant in drier conditions (Fig. 7C). This difference is particularly noticeable between microbes with inducible

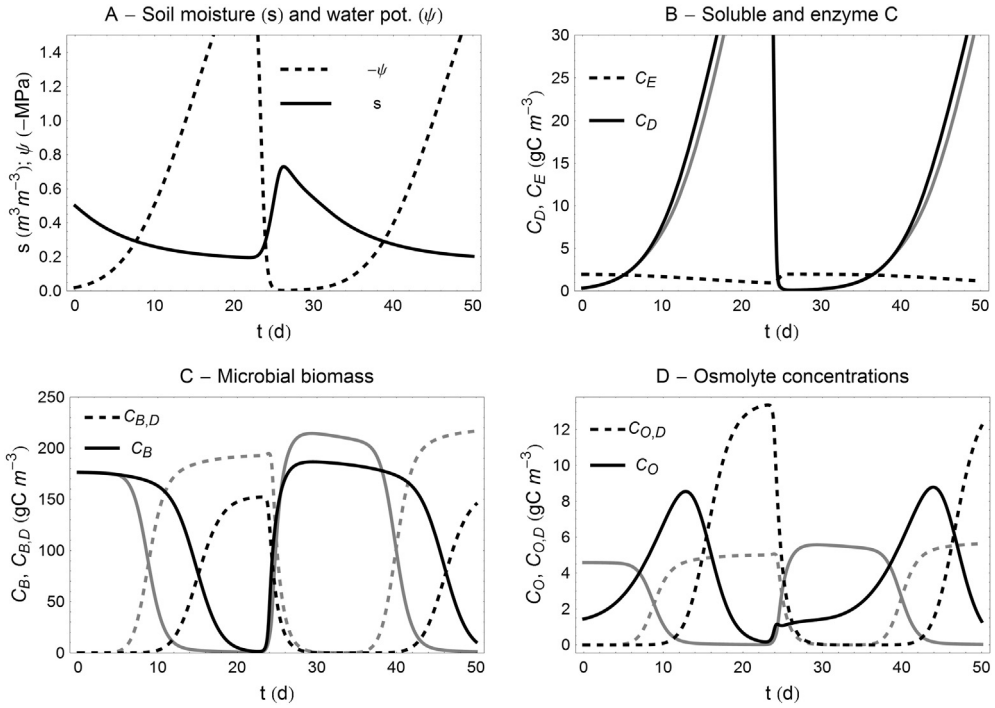

Fig. 5. Behavior of modeled soil C compartments during two drying-wetting cycles, for inducible (black curves) and constitutive osmolyte production (gray; only shown in B-D). A) soil moisture (s) and soil water potential (ψ), B) soluble organic C (C_D) and enzyme C (C_E), C) active (C_B) and dormant biomass ($C_{B,D}$), and D) osmolytes associated to active and dormant biomass (C_O and $C_{O,D}$, respectively). Parameter values are reported in Table 2, except $\delta = 10^{-4}$ m, $c_{A\to D} = 0.1$, $C_{E,0} = 5$ gC m^{-3}. The temporal changes of C_S are not shown because at this short time scales they are not significant and C_S can be regarded as an almost constant substrate pool.

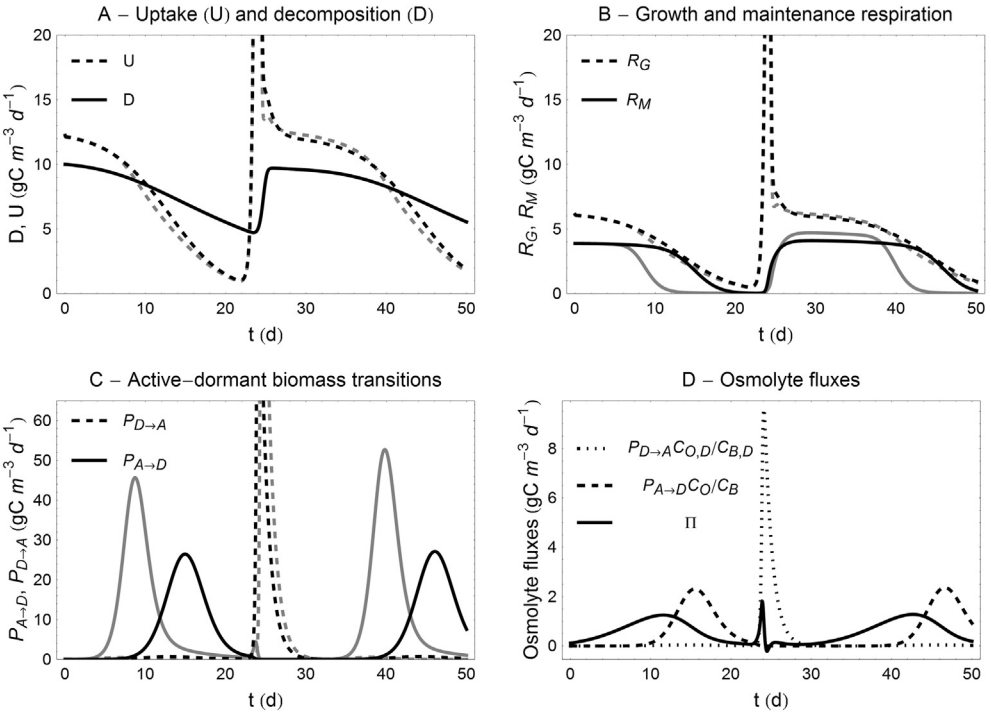

Fig. 6. Behavior of modeled soil C fluxes during two drying-wetting cycles, for inducible (black curves) and constitutive osmolyte production (gray; only shown in A–C). A) decomposition (D) and uptake (U), B) maintenance (R_M) and growth respiration (R_G), C) exchanges of biomass between active and dormant compartments ($P_{A\to D}$ and $P_{D\to A}$), and D) osmolyte production (Π), osmolyte accumulation in dormant biomass ($P_{A\to D}C_O/C_B$), and release upon rewetting from the dormant biomass ($P_{D\to A}C_{O,D}/C_{B,D}$). Parameter values are as in Fig. 5.

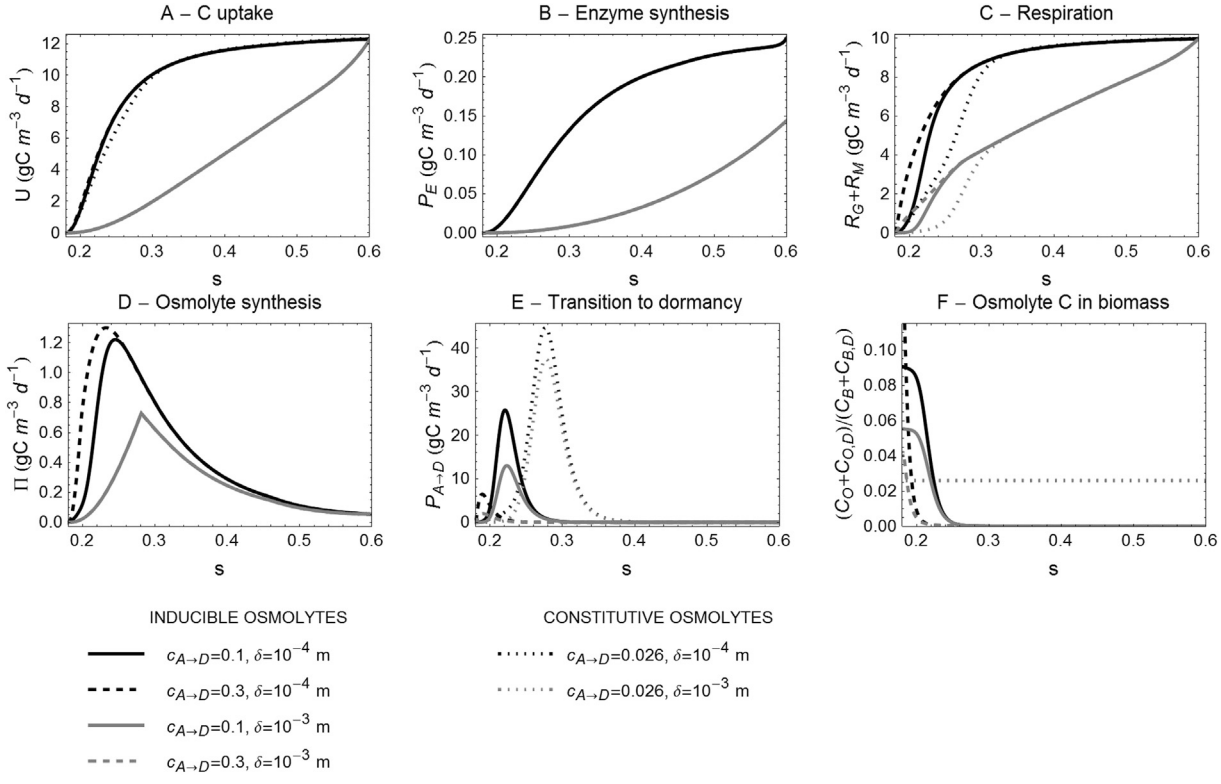

Fig. 7. Selected C fluxes and pools as a function of soil moisture (s) during a prolonged soil dry-down, for different osmoregulation strategies (constitutive *vs*. induced osmolytes), different values of the threshold osmolyte concentration, $c_{A\to D}$, and of the characteristic distance, δ. A) microbial uptake, U; B) enzyme production, P_E; C) total heterotrophic respiration, $R_G + R_M$, D) osmolyte production, Π; E) rate of transition from active to dormant biomass, $P_{A\to D}$; F) ratio of total osmolyte C to total biomass C. Note that solid and dashed lines in A–B are superimposed; parameter values as in Fig. 5, except for δ and $c_{A\to D}$, which are varied as indicated.

(dashed and solid curves) and with constitutive (dotted) osmolytes – the latter switching to the dormant state and slowing respiration at relatively high soil moisture. Hence, different combinations of these microbial traits may alter the shape of the respiration-soil moisture relation.

Different distances between substrates and microbes also alter the relations between soil moisture and C fluxes. A larger δ inhibits mass transfer at any soil moisture level (Equation (25)), resulting in gradual declines of uptake and respiration starting in relatively moist conditions (gray lines in Fig. 7A and C). Moreover, lowered C-supply to the microbes starts limiting osmolyte production (Fig. 7D), which triggers a faster transition to the dormant state, relative to the rate of C uptake (Fig. 7E). Hence, large values of δ (analogous to deeper soils with lower substrate and biomass concentrations, or to stable aggregates un-accessible to microbes) cause respiration to stop earlier during the drying event (i.e., at higher soil moisture) than would occur with a small value of δ.

The sensitivity analysis employing the elasticity of heterotrophic respiration (not shown) largely confirms the patterns shown in Fig. 7. Sensitivities increase as soil moisture decreases, except under extremely dry conditions when C fluxes are practically zero and insensitive to changes in the parameter values. Increases in δ, $c_{A\to D}$, and $C_{E,0}$ respectively cause strong declines ($E_\delta < 0$), strong increases ($E_{cA\to D} > 0$), and moderate increases in respiration ($E_{CE,0} > 0$, but generally smaller in absolute value than E_δ and $E_{cA\to D}$). Interestingly, the effect of $C_{E,0}$ increases when δ is smaller, implying that microbial enzyme synthesis strategies play a role only when substrates are accessible.

Fig. 8 shows the total C exchanged in different processes over an extended dry period, as a function of $c_{A\to D}$ and δ. The lowered C supply when δ is large makes it difficult to invest C in osmolyte production and thus to maintain active microbial cells in dry conditions. As a result, C allocation to osmoregulation may be small for large δ (Fig. 8A), causing lower C uptake as well (Fig. 8B). A limited allocation to C_O is also achieved when the osmolyte concentration triggering dormancy is low, i.e., microbes become dormant at soil moisture levels sufficiently high not to require much osmolyte accumulation. In this case, however, C uptake over the duration of a dry-down is less affected than C investment, because most of the C is taken up when the soil is still moist and most microbes are active (compare Fig. 8A and B at low $c_{A\to D}$). Total respiration exhibits a similar pattern, increasing as $c_{A\to D}$ is increased and δ is decreased (Fig. 8C). As a result, the microbial C balance during this single dry-down (total uptake minus total respiration) is positive only for small values of δ. In contrast, for large δ, the C uptake is too small to support respiration demands and hence the biomass pool decreases.

4. Discussion

4.1. A trait-based approach to modeling microbial responses to drought

Numerous soil C models describe microbial growth and responses to changes in substrate availability (for a review, see Manzoni and Porporato, 2009), including in some cases also explicit representations of substrate diffusion limitations (Allison, 2005; Ginovart et al., 2005; Davidson et al., 2012; Resat et al., 2012), or dormancy (Blagodatsky and Richter, 1998; Bär et al., 2002; Resat et al., 2012). Here we propose a model that couples an approximated representation of diffusion limitations due to low moisture content to a description of osmoregulation, dormancy, and extracellular enzyme synthesis in soil microbes, thus offering an integrated modeling platform to assess microbial responses to changes in moisture. In the proposed model, physiological and physical factors are clearly separated. Equation (9) describes changes in the uptake rate due to diffusion limitations, but it does not capture the physiological responses to water stress, which are instead modeled by the osmoregulatory, dormancy/reactivation, and enzyme synthesis mechanisms (Sections 2.2, 2.3, and 2.4).

Different from previous models, microbial responses to moisture changes are encoded in a set of parameters that represent specific eco-physiological traits. The variation of these traits in a community mirrors long-term strategies adopted to cope with a given environment (Allison, 2012; Lennon et al., 2012; Schimel and Schaeffer, 2012; Wallenstein and Hall, 2012; Evans and Wallenstein, 2013). Having these microbial traits and strategies clearly encoded into model parameters allows developing mathematical theories to explain observed patterns and to produce new hypotheses. Our results indeed suggest that different strategies may cause different patterns in C cycling during dry periods, affecting the predicted community-level relations between soil moisture and substrate consumption, enzyme production, respiration, dormancy/reactivation, and total osmolyte concentration in microbial biomass (Fig. 7). This variability of the biogeochemical responses to drying and rewetting cannot be captured by simpler models that use empirical moisture-dependent rate modifiers (Rodrigo et al., 1997; Bauer et al., 2008). The downside of the proposed representation is an increase in model complexity that might require support from specific empirical studies – e.g., assessing osmolyte concentrations

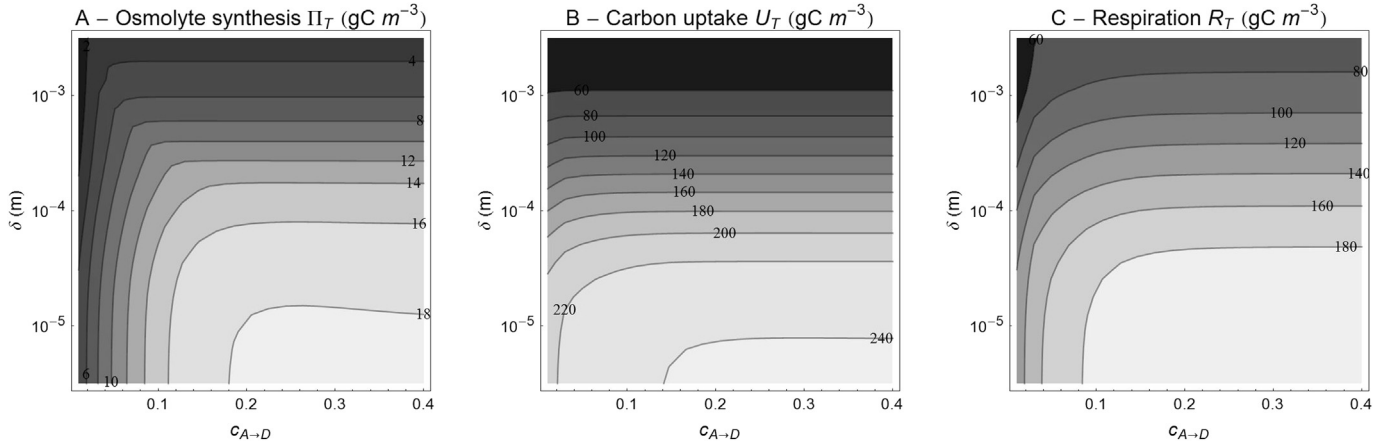

Fig. 8. A) Total amount of C invested in inducible osmolytes (denoted by Π_T), B) total C uptake (U_T), and C) total respiration (R_T, including maintenance and growth components) during a 20 day soil drying event for different combinations of the threshold osmolyte concentration, $c_{A\to D}$, and the microbe-substrate distance δ. Other parameters are as in Fig. 5.

or identification of the dormant *vs.* active fractions of the microbial biomass.

4.2. Alternative life-history strategies to cope with moisture changes

The developed model captures community-level responses, assuming that the model parameters are representative of the mean microbial traits in a given community. Hence, variations in response strategies can be interpreted as changes in the mean community response, as it would occur, e.g., across soil types or climatic conditions. Nevertheless, model results can be used to define a set of life-history strategies, based on different combinations of microbial parameters (Fig. 9). A similar trait-based characterization has been proposed between microbial producers *vs.* cheaters (Allison, 2005), among microbes adopting different strategies of resource acquisition (Allison, 2012), between opportunists *vs.* specialists with regard to C substrates (Moorhead and Sinsabaugh, 2006) or varying environmental conditions (Lennon et al., 2012; Wallenstein and Hall, 2012; Evans and Wallenstein, 2013), and between microbes undergoing dormancy *vs.* tolerating adverse conditions (Bär et al., 2002; Jones and Lennon, 2010). Here we extended these characterizations by fully coupling the dynamics of osmoregulation, enzyme production, and dormancy.

Microbes that tolerate drought by synthesizing osmolytes to buffer changes in soil water potential are able to remain active in dry conditions, thus exploiting the available resources throughout the dry period. Compatible solutes used for osmoregulation also serve other functions, which may play a role in a hypothetical 'optimization' of microbial C economy (Welsh, 2000), although these functions are not considered here for simplicity. However, resources to synthetize osmolytes may be limited by lowered diffusion (Skopp et al., 1990; Manzoni et al., 2012), so that investing large amounts of C for osmoregulation might have relatively small returns (Figs. 8 and 9). Active osmoregulation is thus expected to be of limited utility in mineral soils in dry climates, whereas in litter (where diffusion limitation is less important) it could be more useful. Nitrogen availability (not considered in this study) is also likely to affect drought response strategies, because osmolyte synthesis requires large amount of nitrogen (Schimel et al., 2007; Tiemann and Billings, 2011). It is thus possible that under nitrogen-poor conditions osmoregulation is not feasible. Indeed,

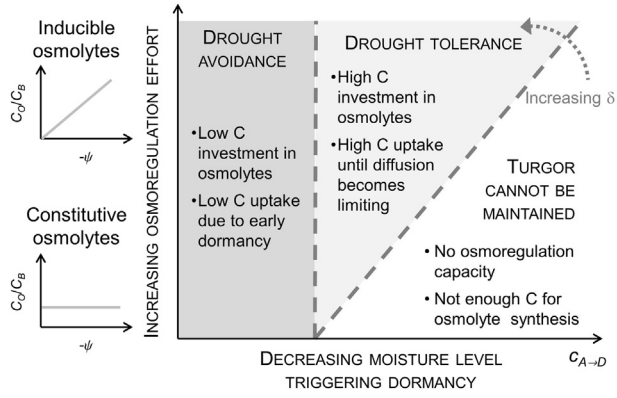

Fig. 9. Conceptual representation of the drought response strategies emerging from different combinations of microbial traits: osmolyte concentration at 50% rate of transition to dormancy on the abscissa and sensitivity of osmoregulation to water availability on the ordinate axis. Shaded areas indicate 'feasible' strategies that allow microbial survival. Increasing the microbe-substrate distance δ decreases C supply (Fig. 7) and thus enlarges the area in which turgor cannot be maintained, regardless of the osmoregulation strategy.

empirical evidence shows that soil microbes often do not accumulate osmolytes during dry periods (Williams and Xia, 2009; Boot et al., 2013; Kakumanu et al., 2013), although other recent studies showed some osmolyte accumulation (Bouskill et al., 2014; Warren, 2014). These results suggest that drought avoidance through dormancy may be a preferred strategy to cope with low water availability – especially in frequently dry or C-poor environments. Indirect support to this hypothesis is provided by evidence of osmoregulation by microbes grown in saline solutions that reach water potential levels comparable to dry soils, but without diffusion limitations (Killham and Firestone, 1984; Schimel et al., 1989; Dotsch et al., 2008; see Fig. 2).

Microbes becoming dormant can avoid dry periods, at the expense of lowered C uptake (Fig. 9). In the model, dormancy may be triggered by large concentrations of osmolytes or lack of C supply to fuel their synthesis (in microbes using inducible osmolytes), or by loss of turgor in microbes that synthesize a constant amount of osmolytes. These triggers are physiologically meaningful, but have not been apparently tested. Model results suggest that a rapid transition to a dormant state triggered by relatively low threshold osmolyte concentrations permits the buildup of a large dormant pool (with its associated osmolytes, see Fig. 4), poised to be reactivated as conditions improve. Relying on dormancy can be a successful strategy as long as reactivation is rapid (Oliver, 2005), so that soluble substrates becoming available upon rewetting can be used, and osmolytes are either effectively metabolized (Tiemann and Billings, 2012) or released fast enough to avoid cell lysis (Halverson et al., 2000; Fierer and Schimel, 2003).

The model results also show that during dry periods, soluble organic C accumulates due to reduced physical losses through leaching and limited consumption by microbes (Zeglin et al., 2013), while extra-cellular enzymatic reactions continue if even at a somewhat reduced rate. Rewetting may transport soluble substrates to the microbial cells, which use it rapidly, causing a pulse in respiration similar to the ones observed in field and laboratory studies (Miller et al., 2005; Muhr et al., 2010; Carbone et al., 2011; Göransson et al., 2013; Meisner et al., 2013; Zeglin et al., 2013). Even though soluble substrates turn over quickly (Bengtson and Bengtsson, 2007), the predicted behavior of this pool seems more dynamic than suggested by some empirical evidence (Göransson et al., 2013). A reason for this discrepancy could be the lack of assimilation regulation (Equation (9)), which could be added by including microbial biomass effect in the uptake function (Ågren and Wetterstedt, 2007). While different microbial traits affect the rate of change in respiration as soil water potential declines (Fig. 7), the amount of C released upon rewetting is less affected (Fig. 6), possibly because all the strategies we considered are characterized by rapid reactivation from dormancy and the same maximum growth rates. Hence, with the current parameterization, the intensity and duration of respiration pulses are largely controlled by the amount of substrate C that has accumulated before rewetting, and hence by the drought duration rather than by being directly affected by microbial physiology; this is consistent with experimental results (Miller et al., 2005; Meisner et al., 2013).

Microbes investing more C in extra-cellular enzymes may also increase the pool of soluble C due to increased rates of decomposition (not shown in the drying–wetting analysis, but illustrated in the steady-state analysis of Fig. 4). Hence, a large C investment in enzymes during a brief active period could be an adaptive strategy to cope with drought (Bouskill et al., 2014). However, larger investment in enzymes may become detrimental as returns diminish (Vetter et al., 1998; Allison, 2012) and the accumulated soluble C is prone to leaching if rewetting is rapid. The overall benefit of investments in enzyme synthesis thus results from both physical factors (duration of dry periods and rainfall intensity) and

biological ones (microbial C balance). A more detailed study exploring the optimality of this strategy under fluctuating moisture conditions is warranted. As the time scale of the investigation is lengthened, changes in microbial community composition (Evans and Wallenstein, 2013; Zeglin et al., 2013) likely alter the community-level traits employed in the model. Moreover, temperature effects that have here been neglected would also start to play a role in the microbial C balance, through effects on enzymatic kinetics, diffusivity, as well as microbial physiology (Ågren and Wetterstedt, 2007; Allison et al., 2010; Davidson et al., 2012).

4.3. Conclusions

A process-based model of soil C cycling under varying moisture conditions is developed where microbial traits regulating drought responses and physical limitations to C supply in dry conditions are accommodated. Different combinations of model parameters define a continuum of microbial strategies. Microbes with active osmoregulation may resist drought at the expense of large C investment to osmolytes, whereas microbes with limited osmoregulation can use the available C for growth, albeit over shorter periods (Fig. 9). Dormancy becomes the only option when either osmolyte concentrations in microbial cells become excessive (in organisms with inducible osmolytes) or when turgor drops to zero (in organisms with fixed osmolyte concentration). The timing of dormancy initiation determines for how long during a dry-down microbes can be metabolically active, but not for how long they can actually grow. In fact, an active microbe in dry conditions is unlikely to receive enough substrates to grow due to diffusion limitations. Hence, drought avoidance through dormancy is a useful (and perhaps the only) strategy in mineral soils where C supply constrains growth and osmolyte synthesis.

While both long-term (under steady state conditions) and short-term (drying-wetting) effects of microbial traits on soil C dynamics were investigated, the role of previous soil moisture history has not been accounted for. Microbial life-history strategies could have evolved in response to a distribution of moisture states originating from random rainfall occurrences, rather than to the mean climate as described by our steady state analysis. Thus, the next step to understand patterns in microbial and soil C along climatic gradients (and to project such understanding to future climatic conditions) is the exploration of how stochastic hydroclimatic conditions affect the optimality of these drought-response microbial life-history strategies.

Acknowledgments

We would like to thank two anonymous reviewers for their constructive criticism. S.M. acknowledges financial support through an excellence grant from the Faculty of Natural Resources and Agricultural Sciences, and the vice-chancellor of the Swedish University of Agricultural Sciences. This work was supported in part by the US National Science Foundation (DEB-1145875/1145649, CBET 1033467, EAR 1331846, EAR 1316258), the US Department of Energy (DOE) through the Office of Biological and Environmental Research (BER) Terrestrial Carbon Processes (TCP) program (DE-SC0006967) and the Agriculture and Food Research Initiative from the USDA National Institute of Food and Agriculture (2011-67003-30222).

Appendix A. Soil hydrology

A soil moisture balance is coupled to the soil C model described by Equations (1)–(7) to provide realistic time-varying water availability. The soil moisture balance equation can be written as (Rodriguez-Iturbe and Porporato, 2004),

$$nZ_r\frac{ds}{dt} = I(t) - ET(s) - L(t,s) - Q(t,s), \tag{27}$$

where s is the relative volumetric soil water content, n is the soil porosity, Z_r is the mean rooting depth, I is the rainfall input, ET is the evapotranspiration rate, L is the leakage rate (modeled after Campbell, 1974), and Q represents runoff, modeled as excess saturation. Soil moisture is related to the soil water potential through a water retention curve approximated by $\psi = \psi_{sat}s^{-b}$ (Campbell, 1974). Leaching of enzymes and dissolved organic C is linked to leakage as,

$$L_E = \frac{C_E L(s)}{(sn + \rho_b K_d)Z_r}, \tag{28}$$

$$L_D = \frac{C_D L(s)}{(sn + \rho_b K_d)Z_r}, \tag{29}$$

where the normalization by $(sn + \rho_b K_d)Z_r$ accounts for sorption (Olesen et al., 2001a) and converts the units to obtain a mass flux (gC m^{-3} of soil d^{-1}).

Appendix B. Estimation of the characteristic distance between substrates and microbial cells

In this Appendix, two methods to estimate the characteristic distance between substrates and microbial cells (δ) are presented. The first method assumes that microbial cells or colonies are located in a cubic lattice with side δ. Based on this premise, the long-term mean microbial biomass (indicated by $\overline{C_B}$) can be expressed as a function of the distance δ, which in turn can be computed at a given $\overline{C_B}$ as,

$$\overline{C_B} = \frac{\#\ \text{cells}}{\text{soil volume}} \times \frac{\text{C mass}}{\text{cell}} = \frac{1}{\delta^3} \times (a_2 a_4) \quad \Rightarrow \quad \delta = \left(\frac{a_2 a_4}{\overline{C_B}}\right)^{1/3}, \tag{30}$$

where $a_2 = 0.5$ is the ratio of microbial C to dry weight and a_4 is the dry weight per cell, estimated in the order of $\sim 10^{-13}$ g/cell (Loferer-Krossbacher et al., 1998). Because microbes grow in colonies of 10–100 cells, a_4 is increased up to $\sim 10^{-11}$ g/colony. Considering a range of $\overline{C_B}$ between 2×10^2 and 2×10^4 gC m^{-3} (Cleveland and Liptzin, 2007), we obtain a range of $\delta \sim 3 \times 10^{-5} - 6 \times 10^{-6}$ m.

The second method assumes that δ corresponds to the mean distance between clusters of microbial cells, computed from statistical analyses of thin sections from undisturbed soil cores. Using this approach δ is found in the range between 2×10^{-4} and 10^{-3} m (Nunan et al., 2002, 2003). The upper values in this range are also comparable to the characteristic distances between bulk soil and roots (Manzoni et al., 2013), which are typical sources of organic substrates for soil microbes. Using this method, the estimates of δ are up to two orders of magnitude larger than using the first approach (Equation (30)). The large uncertainty in this parameter calls for a sensitivity analysis over the range between 10^{-5} to 10^{-3} m.

References

Ågren, G.I., Wetterstedt, J.A.M., 2007. What determines the temperature response of soil organic matter decomposition? Soil Biology & Biochemistry 39, 1794–1798.
Allison, S.D., 2005. Cheaters, diffusion and nutrients constrain decomposition by microbial enzymes in spatially structured environments. Ecology Letters 8, 626–635.

Allison, S.D., 2012. A trait-based approach for modelling microbial litter decomposition. Ecology Letters 15, 1058–1070.
Allison, S.D., Wallenstein, M.D., Bradford, M.A., 2010. Soil-carbon response to warming dependent on microbial physiology. Nature Geoscience 3, 336–340.
Austin, A.T., Yahdjian, L., Stark, J.M., Belnap, J., Porporato, A., Norton, U., Ravetta, D.A., Schaeffer, S.M., 2004. Water pulses and biogeochemical cycles in arid and semiarid ecosystems. Oecologia 141, 221–235.
Bär, M., von Hardenberg, J., Meron, E., Provenzale, A., 2002. Modelling the survival of bacteria in drylands: the advantage of being dormant. Proceedings of the Royal Society of London Series B –Biological Sciences 269, 937–942.
Bauer, J., Herbst, M., Huisman, J.A., Weihermuller, L., Vereecken, H., 2008. Sensitivity of simulated soil heterotrophic respiration to temperature and moisture reduction functions. Geoderma 145, 17–27.
Bengtson, P., Bengtsson, G., 2007. Rapid turnover of DOC in temperate forests accounts for increased CO_2 production at elevated temperatures. Ecology Letters 10, 783–790.
Blagodatsky, S.A., Richter, O., 1998. Microbial growth in soil and nitrogen turnover: a theoretical model considering the activity state of microorganisms. Soil Biology & Biochemistry 30, 1743–1755.
Boot, C.M., Schaeffer, S.M., Schimel, J.P., 2013. Static osmolyte concentrations in microbial biomass during seasonal drought in a California grassland. Soil Biology & Biochemistry 57, 356–361.
Borken, W., Matzner, E., 2009. Reappraisal of drying and wetting effects on C and N mineralization and fluxes in soils. Global Change Biology 15, 808–824.
Bouskill, N.J., Baran, R., Wood, T.E., Hao, Z., Ye, Z., Bowen, B.P., Lim, H.C., Zhou, J., Van Nostrand, J.D., Nico, P.S., Holman, H.Y., Gilbert, B., Silver, W.L., Northen, T.R., Brodie, E.L. 2014. Microbial functional response to drought impacts carbon and nutrient cycling of tropical forest soils (in preparation).
Bratbak, G., Dundas, I., 1984. Bacterial dry-matter content and biomass estimations. Applied and Environmental Microbiology 48, 755–757.
Campbell, G.S., 1974. Simple method for determining unsaturated conductivity from moisture retention data. Soil Science 117, 311–314.
Carbone, M.S., Still, C.J., Ambrose, A.R., Dawson, T.E., Williams, A.P., Boot, C.M., Schaeffer, S.M., Schimel, J.P., 2011. Seasonal and episodic moisture controls on plant and microbial contributions to soil respiration. Oecologia 167, 265–278.
Cleveland, C.C., Liptzin, D., 2007. C:N:P stoichiometry in soil: is there a "Redfield ratio" for the microbial biomass? Biogeochemistry 85, 235–252.
Davidson, E.A., Samanta, S., Caramori, S.S., Savage, K., 2012. The Dual Arrhenius and Michaelis-Menten kinetics model for decomposition of soil organic matter at hourly to seasonal time scales. Global Change Biology 18, 371–384.
Dotsch, A., Severin, J., Alt, W., Galinski, E.A., Kreft, J.U., 2008. A mathematical model for growth and osmoregulation in halophilic bacteria. Microbiology-Sgm 154, 2956–2969.
Evans, S.E., Wallenstein, M.D., 2013. Climate change alters ecological strategies of soil bacteria. Ecology Letters 17 (2), 155–164.
Fierer, N., Schimel, J.P., 2003. A proposed mechanism for the pulse in carbon dioxide production commonly observed following the rapid rewetting of a dry soil. Soil Science Society of America Journal 67, 798–805.
Freckman, D.W., 1986. The ecology of dehydration in soil organisms. In: Leopold, A.C. (Ed.), Membranes, Metabolism, and Dry Organisms.
Ginovart, M., Lopez, D., Gras, A., 2005. Individual-based modelling of microbial activity to study mineralization of C and N and nitrification process in soil. Nonlinear Analysis-Real World Applications 6, 773–795.
Göransson, H., Godbold, D.L., Jones, D.L., Rousk, J., 2013. Bacterial growth and respiration responses upon rewetting dry forest soils: impact of drought-legacy. Soil Biology & Biochemistry 57, 477–486.
Griffin, D.M., 1981. Water and microbial stress. Advances in Microbial Ecology 5, 91–136.
Halverson, L.J., Jones, T.M., Firestone, M.K., 2000. Release of intracellular solutes by four soil bacteria exposed to dilution stress. Soil Science Society of America Journal 64, 1630–1637.
Hamamoto, S., Moldrup, P., Kawamoto, K., Komatsu, T., 2010. Excluded-volume expansion of Archie's law for gas and solute diffusivities and electrical and thermal conductivities in variably saturated porous media. Water Resources Research 46.
Jones, S.E., Lennon, J.T., 2010. Dormancy contributes to the maintenance of microbial diversity. Proceedings of the National Academy of Sciences of the United States of America 107, 5881–5886.
Jones, D.L., Healey, J.R., Willett, V.B., Farrar, J.F., Hodge, A., 2005. Dissolved organic nitrogen uptake by plants - an important N uptake pathway? Soil Biology & Biochemistry 37, 413–423.
Kakumanu, M.L., Cantrell, C.L., Williams, M.A., 2013. Microbial community response to varying magnitudes of desiccation in soil: a test of the osmolyte accumulation hypothesis. Soil Biology & Biochemistry 57, 644–653.
Kayingo, G., Kilian, S.G., Prior, B.A., 2001. Conservation and release of osmolytes by yeasts during hypo-osmotic stress. Archives of Microbiology 177, 29–35.
Killham, K., Firestone, M.K., 1984. Salt stress-control of intracellular solutes in Streptomycetes indigenous to saline soils. Applied and Environmental Microbiology 47, 301–306.
Lawrence, C.R., Neff, J.C., Schimel, J.P., 2009. Does adding microbial mechanisms of decomposition improve soil organic matter models? A comparison of four models using data from a pulsed rewetting experiment. Soil Biology & Biochemistry 41, 1923–1934.
Lennon, J.T., Aanderud, Z.T., Lehmkuhl, B.K., Schoolmaster, D.R., 2012. Mapping the niche space of soil microorganisms using taxonomy and traits. Ecology 93, 1867–1879.
Loferer-Krossbacher, M., Klima, J., Psenner, R., 1998. Determination of bacterial cell dry mass by transmission electron microscopy and densitometric image analysis. Applied and Environmental Microbiology 64, 688–694.
Manzoni, S., Porporato, A., 2007. Theoretical analysis of nonlinearities and feedbacks in soil carbon and nitrogen cycles. Soil Biology & Biochemistry 39, 1542–1556.
Manzoni, S., Porporato, A., 2009. Soil carbon and nitrogen mineralization: theory and models across scales. Soil Biology & Biochemistry 41, 1355–1379.
Manzoni, S., Schimel, J.P., Porporato, A., 2012. Responses of soil microbial communities to water stress: results from a meta-analysis. Ecology 93, 930–938.
Manzoni, S., Vico, G., Katul, G., Porporato, A., 2013. Biological constraints on water transport in the soil-plant-atmosphere system. Advances in Water Resources, 292–304.
Meisner, A., Baath, E., Rousk, J., 2013. Microbial growth responses upon rewetting soil dried for four days or one year. Soil Biology & Biochemistry 66, 188–192.
Miller, A.E., Schimel, J.P., Meixner, T., Sickman, J.O., Melack, J.M., 2005. Episodic rewetting enhances carbon and nitrogen release from chaparral soils. Soil Biology & Biochemistry 37, 2195–2204.
Moldrup, P., Olesen, T., Komatsu, T., Schjonning, P., Rolston, D.E., 2001. Tortuosity, diffusivity, and permeability in the soil liquid and gaseous phases. Soil Science Society of America Journal 65, 613–623.
Moorhead, D.L., Sinsabaugh, R.L., 2006. A theoretical model of litter decay and microbial interaction. Ecological Monographs 76, 151–174.
Moorhead, D.L., Lashermes, G., Sinsabaugh, R.L., 2012. A theoretical model of C- and N-acquiring exoenzyme activities, which balances microbial demands during decomposition. Soil Biology & Biochemistry 53, 133–141.
Moyano, F.E., Vasilyeva, N., Bouckaert, L., Cook, F., Craine, J., Yuste, J.C., Don, A., Epron, D., Formanek, P., Franzluebbers, A., Ilstedt, U., Katterer, T., Orchard, V., Reichstein, M., Rey, A., Ruamps, L., Subke, J.A., Thomsen, I.K., Chenu, C., 2012. The moisture response of soil heterotrophic respiration: interaction with soil properties. Biogeosciences 9, 1173–1182.
Moyano, F.E., Manzoni, S., Chenu, C., 2013. Responses of soil heterotrophic respiration to moisture availability: an exploration of processes and models. Soil Biology and Biochemistry 59, 72–85.
Muhr, J., Franke, J., Borken, W., 2010. Drying-rewetting events reduce C and N losses from a Norway spruce forest floor. Soil Biology & Biochemistry. http://dx.doi.org/10.1016/j.soilbio.2010.1003.1024.
Nunan, N., Wu, K., Young, I.M., Crawford, J.W., Ritz, K., 2002. In situ spatial patterns of soil bacterial populations, mapped at multiple scales, in an arable soil. Microbial Ecology 44, 296–305.
Nunan, N., Wu, K.J., Young, I.M., Crawford, J.W., Ritz, K., 2003. Spatial distribution of bacterial communities and their relationships with the micro-architecture of soil. Fems Microbiology Ecology 44, 203–215.
Olesen, T., Gamst, J., Moldrup, P., Komatsu, T., Rolston, D.E., 2001a. Diffusion of sorbing organic chemicals in the liquid and gaseous phases of repacked soil. Soil Science Society of America Journal 65, 1585–1593.
Olesen, T., Moldrup, P., Yamaguchi, T., Rolston, D.E., 2001b. Constant slope impedance factor model for predicting the solute diffusion coefficient in unsaturated soil. Soil Science 166, 89–96.
Oliver, J.D., 2005. The viable but nonculturable state in bacteria. Journal of Microbiology 43, 93–100.
Or, D., Smets, B.F., Wraith, J.M., Dechesne, A., Friedman, S.P., 2007. Physical constraints affecting bacterial habitats and activity in unsaturated porous media - a review. Advances in Water Resources 30, 1505–1527.
Placella, S.A., Brodie, E.L., Firestone, M.K., 2012. Rainfall-induced carbon dioxide pulses result from sequential resuscitation of phylogenetically clustered microbial groups. Proceedings of the National Academy of Sciences of the United States of America 109, 10931–10936.
Potts, M., 1994. Desiccation tolerance of prokaryotes. Microbiological Reviews 58, 755–805.
Raab, T.K., Lipson, D.A., Monson, R.K., 1999. Soil amino acid utilization among species of the Cyperaceae: plant and soil processes. Ecology 80, 2408–2419.
Reichstein, M., Tenhunen, J.D., Roupsard, O., Ourcival, J.M., Rambal, S., Miglietta, F., Peressotti, A., Pecchiari, M., Tirone, G., Valentini, R., 2002. Severe drought effects on ecosystem CO_2 and H_2O fluxes at three Mediterranean evergreen sites: revision of current hypotheses? Global Change Biology 8, 999–1017.
Resat, H., Bailey, V., McCue, L.A., Konopka, A., 2012. Modeling microbial dynamics in heterogeneous environments: growth on soil carbon sources. Microbial Ecology 63, 883–897.
Rodrigo, A., Recous, S., Neel, C., Mary, B., 1997. Modelling temperature and moisture effects on C-N transformations in soils: comparison of nine models. Ecological Modelling 102, 325–339.
Rodriguez-Iturbe, I., Porporato, A., 2004. Ecohydrology of Water-controlled Ecosystems. Soil Moisture and Plant Dynamics. Cambridge University Press, Cambridge.
Schimel, J., Schaeffer, S.M., 2012. Microbial control over carbon cycling in soil. Frontiers in Microbiology 3.
Schimel, J.P., Weintraub, M.N., 2003. The implications of exoenzyme activity on microbial carbon and nitrogen limitation in soil: a theoretical model. Soil Biology & Biochemistry 35, 549–563.

Schimel, J.P., Scott, W.J., Killham, K., 1989. Changes in cytoplasmic carbon and nitrogen pools in a soil bacterium and fungus in response to salt stress. Applied and Environmental Microbiology 55, 1635–1637.
Schimel, J., Balser, T.C., Wallenstein, M., 2007. Microbial stress-response physiology and its implications for ecosystem function. Ecology 88, 1386–1394.
Schjonning, P., Thomsen, I.K., Moldrup, P., Christensen, B.T., 2003. Linking soil microbial activity to water- and air-phase contents and diffusivities. Soil Science Society of America Journal 67, 156–165.
Skopp, J., Jawson, M.D., Doran, J.W., 1990. Steady-state aerobic microbial activity as a function of soil-water content. Soil Science Society of America Journal 54, 1619–1625.
Steinweg, J.M., Dukes, J.S., Wallensteine, M.D., 2012. Modeling the effects of temperature and moisture on soil enzyme activity: linking laboratory assays to continuous field data. Soil Biology & Biochemistry 55, 85–92.
Stolpovsky, K., Martinez-Lavanchy, P., Heipieper, H.J., Van Cappellen, P., Thullner, M., 2011. Incorporating dormancy in dynamic microbial community models. Ecological Modelling 222, 3092–3102.
Tiemann, L.K., Billings, S.A., 2011. Changes in variability of soil moisture alter microbial community C and N resource use. Soil Biology & Biochemistry 43, 1837–1847.
Tiemann, L.K., Billings, S.A., 2012. Tracking C and N flows through microbial biomass with increased soil moisture variability. Soil Biology & Biochemistry 49, 11–22.
Toberman, H., Evans, C.D., Freeman, C., Fenner, N., White, M., Emmett, B.A., Artz, R.R.E., 2008. Summer drought effects upon soil and litter extracellular phenol oxidase activity and soluble carbon release in an upland Calluna heathland. Soil Biology & Biochemistry 40, 1519–1532.
Vetter, Y.A., Deming, J.W., Jumars, P.A., Krieger-Brockett, B.B., 1998. A predictive model of bacterial foraging by means of freely released extracellular enzymes. Microbial Ecology 36, 75–92.
Wallenstein, M.D., Hall, E.K., 2012. A trait-based framework for predicting when and where microbial adaptation to climate change will affect ecosystem functioning. Biogeochemistry 109, 35–47.
Warren, C.R., 2014. Response of osmolytes in soil to drying and rewetting. Soil Biology & Biochemistry 70, 22–32.
Welsh, D.T., 2000. Ecological significance of compatible solute accumulation by micro-organisms: from single cells to global climate. Fems Microbiology Reviews 24, 263–290.
Williams, M.A., Xia, K., 2009. Characterization of the water soluble soil organic pool following the rewetting of dry soil in a drought-prone tallgrass prairie. Soil Biology & Biochemistry 41, 21–28.
Zeglin, L.H., Bottomley, P.J., Jumpponen, A., Rice, C.W., Arango, M., Lindsley, A., McGowan, A., Mfombep, P., Myrold, D.D., 2013. Altered precipitation regime affects the function and composition of soil microbial communities on multiple time scales. Ecology 94, 2334–2345.